

Received March 18, 2021, accepted April 8, 2021, date of publication April 16, 2021, date of current version April 23, 2021.

Digital Object Identifier 10.1109/ACCESS.2021.3073735

Helical Long Period Fiber Grating Incribed in Elliptical Core Polarization-Maintaining Fiber

CAILING FU, PENGFEI LI, ZHIYONG BAI^{1b}, AND YIPING WANG^{1b}, (Senior Member, IEEE)

Key Laboratory of Optoelectronic Devices and Systems of Ministry of Education and Guangdong Province, College of Physics and Optoelectronic Engineering, Shenzhen University, Shenzhen 518060, China

Shenzhen Key Laboratory of Photonic Devices and Sensing Systems for Internet of Things, Guangdong and Hong Kong Joint Research Centre for Optical Fibre Sensors, Shenzhen University, Shenzhen 518060, China

Corresponding author: Yiping Wang (ypwang@szu.edu.cn)

This work was supported in part by the National Natural Science Foundation of China (NSFC) under Grant 61635007 and Grant 61905155; in part by the Natural Science Foundation of Guangdong Province under Grant 2019A050510047, Grant 2019B1515120042, and Grant 2021A1515011925; and in part by the Shenzhen Key Laboratory of Photonic Devices and Sensing Systems for Internet of Things.

ABSTRACT A high-quality helical long period fiber grating (HLPFG) in elliptical core polarization-maintaining fiber (PMF) was experimentally demonstrated by using the hydrogen-oxygen flame heating technique. Such a single HLPFG with a length of 6.5 mm could be used to generate orbital angular momentum (OAM) modes, i.e., $OAM_{\pm 2}$. The secret of the successful generation of the $OAM_{\pm 2}$ mode is that the elliptical core PMF has two-fold symmetry in the cross-section. The resonance dip of the coupling attenuation and wavelength was strongly dependent on the length and helical pitch of the HLPFG. The HLPFG also exhibited a higher strain sensitivity of 30.7 pm/ $\mu\epsilon$. The proposed method opens a new way to generate a higher-order OAM mode by using multiple-fold symmetry fiber.

INDEX TERMS Fiber gratings, optical fiber sensors, optical fiber communication.

I. INTRODUCTION

Helical long period fiber gratings (HLPFGs) with periodic screw-type refractive index (RI) modulation along the fiber axis in single mode fiber (SMF) [1]–[3], few mode fiber (FMF) [4], [5], multi-core fiber [6], photonic crystal fiber (PCF) [7]–[10], photonic band-gap fiber (PBF) [11], and polarization-maintaining fiber (PMF) [12] have been fabricated and demonstrated by using the CO₂ laser irradiation, electric arc discharge, and hydrogen-oxygen flame heating technique. These HLPFGs in different types of fibers have been widely used as orbital angular momentum (OAM) mode generator, filter [13], [14], and fiber sensor [15]–[17] attributing to its unique advantages, such as the low polarization dependence loss (PDL) and the inherent helical-phase. As being an OAM mode generator, low-order and high-order OAM modes have been successfully demonstrated and generated by using HLPFG in SMF [1], FMF [4], [5], and PCF [7], [10] without any external components. High-order OAM mode, i.e., greater than $OAM_{\pm 1}$ mode, have been experimentally reported by HLPFGs in FMF and PCF. Moreover, the effect of the fiber core symmetry on the topological charge of the generated OAM modes has been simulated by

various approaches, such as coupled-mode theory, spin-orbit interaction Hamiltonians, and perturbation theory [1]–[21]. For example, Alexeyev *et al.* theoretically demonstrated that a HLPFG with N-fold rotation symmetry had an ability to change the topological charge of the incoming field by N units, i.e., generating $OAM_{\pm N}$ modes [18], which was also suitable for the HLPFG in elliptical core fiber [20], theoretically indicating that $OAM_{\pm 2}$ modes could be generated by the HLPFG in elliptical core fiber with two-fold rotation symmetry. Besides, Xu *et al.* also demonstrated that a HLPFG with N-fold symmetry in the cross section could generate $OAM_{\pm N}$ and $OAM_{\pm(N\pm 2)}$ modes, rather than only $OAM_{\pm N}$ modes [21]. The afore-mentioned established simulation selection rules on the topological charge of the generated OAM modes are different with each other, but few experiments have been conducted to verify it. The HLPFG in elliptical core PMF with two-fold rotation symmetry could be used to investigate the characteristics of the generated OAM modes. Besides, the HLPFGs have been used as torsion [6], [11], [9], and current sensor [15] due to its periodic screw-type structure, while the strain properties of the HLPFG have not been drawn attention yet.

In this letter, we experimentally fabricated an HLPFG in elliptical core PMF with two-fold symmetry in the cross-section by use of the hydrogen-oxygen flame heating

The associate editor coordinating the review of this manuscript and approving it for publication was Yang Yue^{1b}.

technique. The effect of the length and helical pitch on the transmission spectrum was investigated experimentally. The second-order mode, i.e., $OAM_{\pm 2}$ mode, has been successfully generated by using such a single HLPFG due to its two-fold symmetry in the cross-section. Moreover, the strain, and torsion properties of the HLPFG were also experimentally investigated.

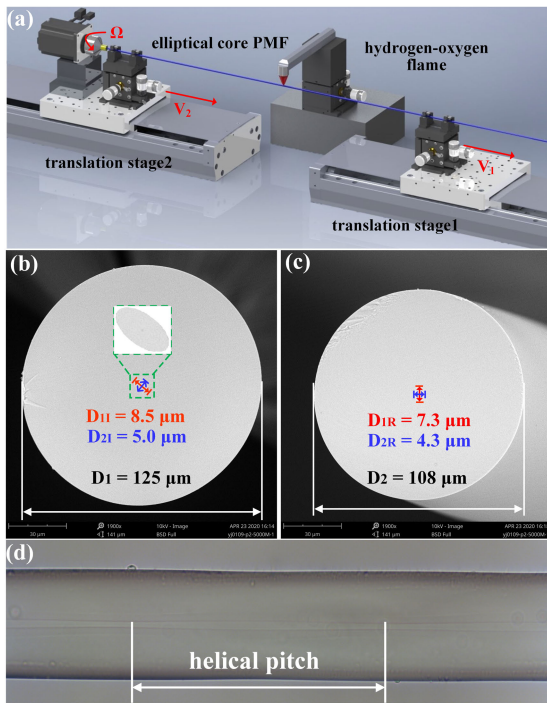


FIGURE 1. (a) Schematic diagram of H-LPFG inscription by use of the hydrogen-oxygen heating technique [9]; Scanning electron micrographs of the cross section of (b) untwisted elliptical core polarization-maintaining fiber (PMF) and (c) twisted sample, i.e., HLPFG in elliptical-core PMF; (d) side-view microscope image of the obtained HLPFG. Inset: enlarged view of the elliptical core for the PMF.

II. EXPERIMENTAL RESULTS AND DISCUSSIONS

An experimental setup, as illustrated in Fig. 1(a), consisting of a fiber rotation motor, two translation stages, and a hydrogen-oxygen flame generator, was used to fabricate HLPFG by use of the hydrogen-oxygen heating technique [9]. An elliptical core PMF (P1C13-125-U25, YOEC) with two-fold symmetry in the cross-section was employed to fabricate the HLPFG. As shown in Fig. 1(b), the initial size of the elliptical core along the major and minor axes is 8.5 and 5.0 μm , respectively. As for fabricating a high-quality HLPFG in the elliptical core PMF, the vital parameters are the velocity of the translation stage1 and stage2, i.e., v_1 and v_2 , the flow rate of the hydrogen-oxygen flame, i.e., Q , and the rotational speed of the fiber rotation motor, i.e., Ω , respectively. The uniformity of the obtained HLPFG was dependent on the flow rate of the hydrogen-oxygen flame, and the helical pitch could be calculated by the equation $\Lambda = 60v_1/\Omega$. In the experiment, v_1 , v_2 , and Q were set as 1.60, 1.38 mm/s and 230, respectively. After twisting the fiber with a rotational

speed of $\Omega = 178$ rpm, a HLPFG in elliptical core PMF with a helical pitch of $\Lambda = 539.3$ μm was obtained, as illustrated in Fig. 1(d). Compared with the HLPFG in standard SMF without physical deformation [9], the HLPFG in elliptical core PMF exhibited an obviously periodic refractive index modulation in the core, where the shape profile was similar to a tapered fiber with bi-taper during one helical period due to its intrinsic major and minor axes structure [28]. In addition, the size of the major and minor axes in the middle of the HLPFG was reduced to 7.3 and 4.3 μm , respectively, and the cladding diameter was also reduced from 125 to 108 μm , as illustrated in Fig. 1(c), attributing to the velocity difference between two translation stages.

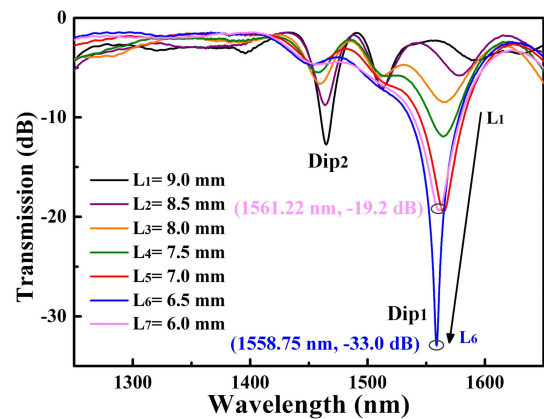


FIGURE 2. Transmission spectrum evolution of the HLPFG in elliptical core PMF with the grating length decrease from L_1 to L_7 , i.e., 9.0 to 6.0 mm, with a step of 0.5 mm.

To measure the transmission spectrum of the HLPFG in elliptical core PMF, a HLPFG sample with a helical pitch of 539.3 μm was cut gradually from L_1 to L_7 , i.e., 9.0 to 6.0 mm, with a step of 0.5 mm. Each end of the achieved HLPFGs was spliced with SMF to measure the transmission spectrum by use of a broadband light source and an optical spectrum analyzer. As shown in Fig. 2, two resonance dips, i.e., Dip₁ and Dip₂, were observed within the wavelength range from 1250 to 1650 nm. As for Dip₁, the resonant wavelength shifted toward a shorter wavelength, and the coupling attenuation increased gradually with the decreased grating length from 9.0 to 6.5 mm. A strong resonant dip of 33.0 dB at the wavelength of 1558.75 nm could be achieved by a length of 6.5 mm, which is approximately 12 times of the helical pitch, i.e., 539.3 μm . The attenuation of the Dip₁ would be increased and then decreased gradually as the length of HLPFG decreased [10]. As shown in Fig. 2, when the length of HLPFG was decreased to 6.0 mm, the attenuation of the Dip₁ was decreased to 19.0 dB at the wavelength of 1561.2 nm, indicating that an optimal coupling attenuation could be achieved by 12 grating periods, i.e., 6.5 mm.

Moreover, the polarization dependent loss (PDL) of the fabricated HLPFG with a helical pitch of 539.3 μm , i.e., $\Omega = 178$ rpm, in elliptical core PMF was measured by

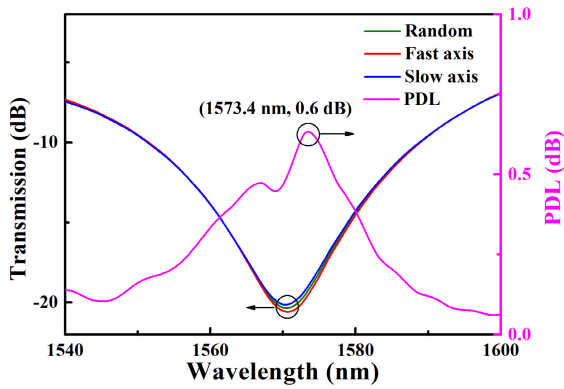


FIGURE 3. Measured transmission spectra and PDL of the obtained HLPFG in elliptical core PMF with a helical pitch of 539.3 μm .

use of a tunable laser, a polarization synthesizer and an optical power meter. As shown in Fig. 3, the transmission spectra at random state, the fast and slow axes are almost completely overlapped, exhibiting a lower PDL of 0.6 dB. The measured result is different from that of a high PDL of the HLPFG fabricated by CO₂ laser in the PMF with two stress applying parts [19]. The reason is that the helical refractive index was induced on the fiber surface, not the core by this method, resulting in asymmetric azimuthal profile.

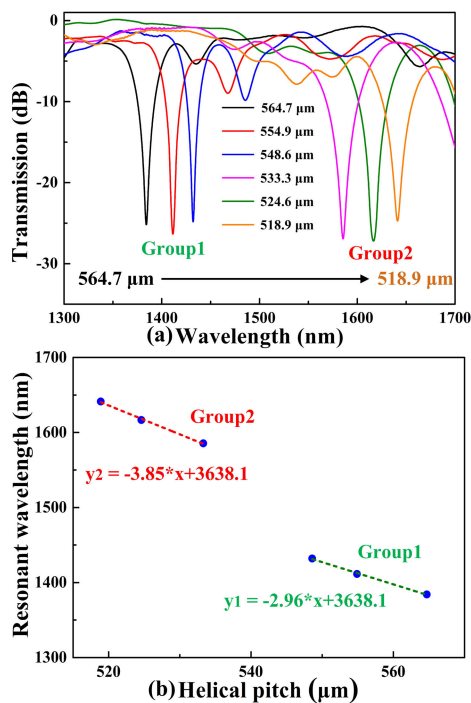


FIGURE 4. (a) Transmission spectra of six HLPFG samples fabricated in elliptical core PMF with a helical pitch of 564.7, 554.9, 548.6, 533.3, 524.6, and 518.9 μm , respectively; (b) measured resonant wavelengths versus the helical pitch of the obtained HLPFGs.

To investigate the effect of the helical pitch on the resonant wavelength, six HLPFGs in elliptical core PMF with a helical pitch of 564.7, 554.9, 548.6, 533.3, 524.6, and 518.9 μm , were fabricated by applying a rotational speed of 170, 173, 175, 180, 183, and 185 rpm, respectively. As shown in Fig. 4(a), the resonance dip, i.e., Dip₁, for

each HLPFG sample has a coupling attenuation of more than 25 dB and an insertion loss of 2.5 dB. The measured resonant wavelength as a function of the helical pitch was not changed continuously, but being divided into two groups, i.e., Group1 and Group2, where the phenomenon is different from the HLPFG in standard SMF, PCF, and all-solid PBF [9], [10], [18]. As for Group1, i.e., with the decrease of the helical pitch from 564.7 to 548.6 μm , the measured resonant wavelength shifted linearly toward a longer wavelength with a smaller slope of -2.96 , while for Group2, i.e., from 533.3 to 518.9 μm , shifted linearly to a longer wavelength with a larger slope of -3.85 , as illustrated by the dotted green and red curve in Fig. 4(b), respectively. The phenomenon, i.e., un-continuous change of the Dip₁ versus the helical pitch, combined with the measured low PDL in Fig. 3, may be due to different cladding modes excited by Group1 and Group2.

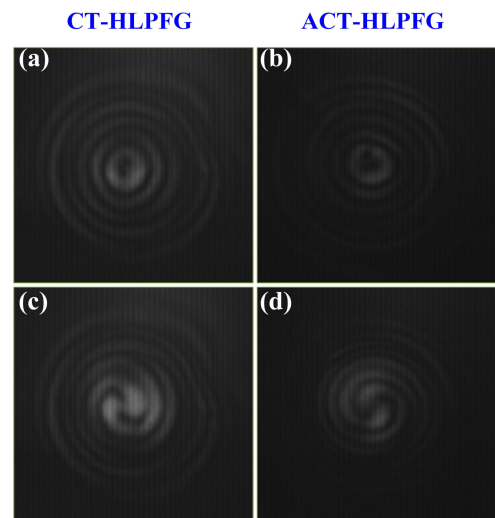


FIGURE 5. (a-b) Beam profiles and (c-d) interference patterns of the OAM₊₂ and OAM₋₂ modes generated by the CT-HLPFG and ACT-HLPFG fabricated in elliptical core PMF, respectively.

Note that afore-obtained experimental data are all from the clockwise-twisted HLPFG (CT-HLPFG) in elliptical core PMF. To measure the beam profile and interference pattern, another type of HLPFG, i.e., anticlockwise-twisted (ACT-HLPFG), was also fabricated with the same fabrication parameters but different rotation directions. An experimental setup illustrated in [10], consisting of reference and sample parts, was used to measure the beam profiles and interference patterns of the two types of HLPFG in elliptical core PMF, i.e., CT-HLPFG and ACT-HLPFG. In the experiment, light from a tunable laser was tuned to the resonant wavelength of the tested HLPFG sample. And the light was split into two parts: one part was sequentially propagated into the tested HLPFG, an objective lens, and a beam splitter, while the other was used as a reference part through an attenuator, and then gathered by use of the beam splitter (BS). The tested HLPFG sample was cleaved at the last period to measure the beam profile. As shown in Figs. 5(a) and 5(b), the beam profile of the CT-HLPFG

and ACT-HLPFG in elliptical core PMF exhibited similar donut-like patterns in the center, i.e., phase singularity, by use of an infrared camera. To verify the properties of the helical phase, the OAM modes generated by the CT-HLPFG and ACT-HLPFG were interfered with the reference light, respectively. As shown in Figs. 5(c) and 5(d), the spiral interference patterns for the OAM_{+2} and OAM_{-2} mode were clearly observed for the CT-HLPFG and ACT-HLPFG in elliptical core PMF, respectively, around the resonant wavelength, indicating that $OAM_{\pm 2}$ modes could be successfully generated by the HLPFG in elliptical core fiber with two-fold symmetry, in good agreement with the simulation that the long-period twisted elliptical fiber with two-fold rotational symmetry possessed the ability to change the incoming Gaussian beam to charge-2 optical vortices in a certain wavelength range [24], [25]. The experimental results verified that the two-fold symmetry fiber, i.e., elliptical core PMF, could only generate the $OAM_{\pm 2}$ modes, rather than $OAM_{\pm 2}$ and $OAM_{\pm 4}$ modes [26]. Moreover, as the $OAM_{\pm 6}$ and $OAM_{\pm 2}$ modes were generated by the helical PCF and HLPFG in elliptical core PMF with two-fold and six-fold symmetry rotational fiber, respectively, indicating that a high-order OAM mode could be generated by choosing multiple-fold symmetry fiber.

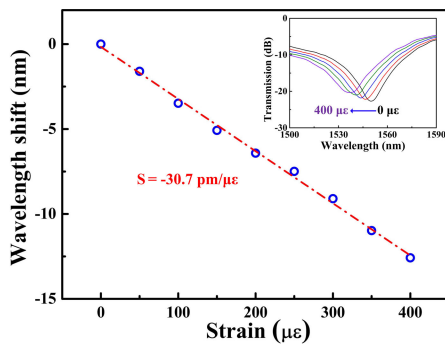


FIGURE 6. Measured resonant wavelength shift as a function of the strain. Inset: transmission spectrum evolution of the HLPFG while the strain increased from 0 to 400 $\mu\epsilon$.

The sensing properties of the HLPFG in elliptical core PMF have also been investigated. Firstly, the strain response was experimentally measured and demonstrated. The two ends of the HLPFG sample were glued and fixed on a holder and a translation stage, where the strain was applied by adjusting the translation stage. The inset is the transmission spectrum evolution of the HLPFG with the strain increased from 0 to 400 $\mu\epsilon$ with a step of 50 $\mu\epsilon$. In the experiment, the HLPFG sample was damaged when a higher strain, i.e., 450 $\mu\epsilon$ was applied. As shown in Fig. 6, with the increase of the strain, the resonant wavelength shifted linearly toward a shorter wavelength with a sensitivity of 30.7 $\text{pm}/\mu\epsilon$, which is one order of magnitude higher than that, i.e., 1.41 [29], and 3.2 $\text{pm}/\mu\epsilon$ [30], of the HLPFGs in the SMF, and PCF by means of hydrogen-oxygen flame heating technique, attributing to the bi-taper shape profile in the core.

Finally, the mechanical torsion response of the HLPFG in elliptical core PMF was investigated by means of fixing two ends of the fiber sample by use of a fiber rotator and fiber holder, respectively, where the distance between two fixed points, i.e., L , is 150 mm. During the measurement, the fiber rotator was clockwise or anti-clockwise rotated from 0° to 360° with a step of 30° , i.e., the mechanical torsion rate of α_M varies from +0.0419 to -0.0419 rad/mm according to the equation of $\alpha_M = \theta/L$. Note that $\alpha_M > 0$ represented the clockwise torsion direction, while $\alpha_M < 0$ was the anti-clockwise torsion direction. As shown in Fig. 7, the resonant wavelength shifted linearly toward a longer wavelength with the increased external mechanical torsion rate under the clockwise mechanical torsion, while the opposite process occurred under the anti-clockwise mechanical torsion. The total wavelength shift was approximately 29.9 nm, and the original spectrum, i.e., $\alpha_M = 0$, was marked in blue. As shown in Fig. 7, the measured torsion sensitivity of the HLPFG in elliptical core PMF was 350.48 $\text{nm}/(\text{rad}\cdot\text{mm}^{-1})$.

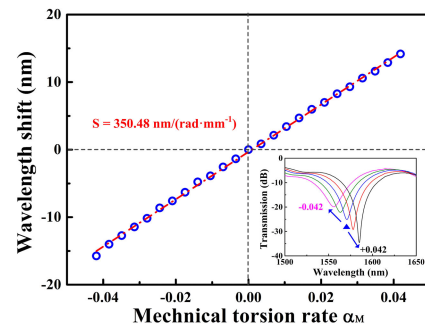


FIGURE 7. Measured resonant wavelength shift as a function of the mechanical torsion rate. Inset: transmission spectrum evolution of HLPFG while mechanical torsion rate, α_M , varies from -0.0419 to $+0.0419$ rad/mm.

III. CONCLUSION

In conclusion, we experimentally demonstrated a novel $OAM_{\pm 2}$ mode generator based on a single HLPFG in elliptical core PMF by use of hydrogen-oxygen flame heating technique. The successful generation of the $OAM_{\pm 2}$ mode was attributed to the two-fold rotation symmetry of the HLPFG in elliptical core PMF. The proposed method opens a new way to generate a higher-order OAM mode by using multiple-fold symmetry fiber. The resonance dip of the coupling attenuation and wavelength was strongly dependent on the length and helical pitch of the HLPFG. Moreover, the HLPFG exhibited a high strain sensitivity of 30.7 $\text{pm}/\mu\epsilon$. Hence, such an HLPFG also could be used to develop a promising high-sensitivity strain sensor.

REFERENCES

- [1] J. Wang, "Advances in communications using optical vortices," *Photon. Res.*, vol. 4, no. 5, pp. B14–B28, Oct. 2016.
- [2] Z. Shen, L. Su, and X. C. Yuan, "Trapping and rotating of a metallic particle trimer with optical vortex," *Appl. Phys. Lett.*, vol. 109, no. 24, p. 109, Dec. 12, 2016.
- [3] A. S. Ostrovsky, C. Rickenstorff-Parrao, and V. Arrizon, "Generation of the 'perfect' optical vortex using a liquid-crystal spatial light modulator," *Opt. Lett.*, vol. 38, no. 4, pp. 534–536, Feb. 15, 2013.

- [4] X. Zhang, A. Wang, R. Chen, Y. Zhou, H. Ming, and Q. Zhan, "Generation and conversion of higher order optical vortices in optical fiber with helical fiber Bragg gratings," *J. Lightw. Technol.*, vol. 34, no. 10, pp. 2413–2418, May 15, 2016.
- [5] Y. Zhao, Z. Liu, and Y. Liu, "Ultra-broadband fiber mode converter based on apodized phase-shifted long-period gratings," *Opt. Lett.*, vol. 44, no. 24, pp. 5905–5908, Dec. 15, 2019.
- [6] S. H. Li, Q. Mo, X. Hu, C. Du, and J. Wang, "Controllable all-fiber orbital angular momentum mode converter," *Opt. Lett.*, vol. 40, no. 18, pp. 4376–4379, Sep. 2015.
- [7] W. Zhang, K. Wei, L. Huang, D. Mao, B. Jiang, and F. Gao, "Optical vortex generation with wavelength tunability based on an acoustically-induced fiber grating," *Opt. Exp.*, vol. 24, pp. 19278–19285, Aug. 2016.
- [8] S. Wu, Y. Li, L. Feng, X. Zeng, W. Li, J. Qiu, Y. Zuo, X. Hong, H. Yu, R. Chen, I. P. Giles, and J. Wu, "Continuously tunable orbital angular momentum generation controlled by input linear polarization," *Opt. Lett.*, vol. 43, no. 9, p. 2130, 2018.
- [9] C. Fu, B. Yu, Y. Wang, S. Liu, Z. Bai, J. He, C. Liao, Y. Wang, Z. Li, Y. Zhang, and K. Yang, "Orbital angular momentum mode converter based on helical long period fiber grating inscribed by hydrogen–oxygen flame," *J. Lightw. Technol.*, vol. 36, no. 9, pp. 1683–1688, May 1, 2018.
- [10] C. Fu, S. Liu, Y. Wang, Z. Bai, J. He, C. Liao, and Y. Zhang, "High-order orbital angular momentum mode generator based on twisted photonic crystal fiber," *Opt. Lett.*, vol. 43, no. 8, pp. 1786–1789, Apr. 2018.
- [11] G. K. L. Wong, M. S. Kang, H. W. Lee, F. Biancalana, C. Conti, T. Weiss, and P. S. J. Russell, "Excitation of orbital angular momentum resonances in helically twisted photonic crystal fiber," *Science*, vol. 337, no. 6093, pp. 446–449, Jul. 2012.
- [12] X. M. Xi, G. Wong, M. H. Frosz, F. Babic, and G. Ahmed, "Orbital-angular-momentum-preserving helical Bloch modes in twisted photonic crystal fiber," *Optica*, vol. 1, no. 3, pp. 165–169, Sep. 2014.
- [13] Y. Zhang, Z. Bai, C. Fu, S. Liu, J. Tang, J. Yu, and C. Liao, "Polarization-independent orbital angular momentum generator based on a chiral fiber grating," *Opt. Lett.*, vol. 44, pp. 61–64, Jan. 2019.
- [14] H. Zhao, P. Wang, T. Yamakawa, and H. Li, "All-fiber second-order orbital angular momentum generator based on a single-helix helical fiber grating," *Opt. Lett.*, vol. 44, no. 21, pp. 5370–5373, Nov. 2019.
- [15] B. Sun, W. Wei, C. Liao, L. Zhang, Z. Zhang, M.-Y. Chen, and Y. Wang, "Automatic arc discharge-induced helical long period fiber gratings and its sensing applications," *IEEE Photon. Technol. Lett.*, vol. 29, no. 11, pp. 873–876, Jun. 1, 2017.
- [16] X. Xi, G. K. L. Wong, T. Weiss, and P. S. J. Russell, "Measuring mechanical strain and twist using helical photonic crystal fiber," *Opt. Lett.*, vol. 38, no. 24, pp. 5401–5404, Dec. 2013.
- [17] S. Xiang, H. Xiongwei, Y. Luyun, and D. Nengli, "Helical long-period grating manufactured with a CO₂ laser on multicore fiber," *Opt. Exp.*, vol. 25, no. 9, pp. 10405–10412, May 2017.
- [18] J. Li, P. Fan, L.-P. Sun, C. Wu, and B.-O. Guan, "Few-period helically twisted all-solid photonic bandgap fibers," *Opt. Lett.*, vol. 43, no. 4, pp. 655–658, Feb. 2018.
- [19] C. Jiang, Y. Liu, Y. Zhao, C. Mou, and T. Wang, "Helical long-period gratings inscribed in polarization-maintaining fibers by CO₂ laser," *J. Lightw. Technol.*, vol. 37, no. 3, pp. 889–896, Feb. 1, 2019.
- [20] C. Zhu, T. Yamakawa, H. Zhao, and H. Li, "All-fiber circular polarization filter realized by using helical long-period fiber gratings," *IEEE Photon. Technol. Lett.*, vol. 30, no. 22, pp. 1905–1908, Nov. 15, 2018.
- [21] C. Zhu, H. Zhao, P. Wang, R. Subramanian, and H. Li, "Enhanced flat-top band-rejection filter based on reflective helical long-period fiber gratings," *IEEE Photon. Technol. Lett.*, vol. 29, no. 12, pp. 964–966, Jun. 15, 2017.
- [22] R. Gao, Y. Jiang, and L. Jiang, "Multi-phase-shifted helical long period fiber grating based temperature-insensitive optical twist sensor," *Opt. Exp.*, vol. 22, no. 13, pp. 15697–15709, Jun. 2014.
- [23] R. Beravat, G. K. L. Wong, and X. M. Xi, "Current sensing using circularly birefringent twisted solid-core photonic crystal fiber," *Opt. Lett.*, vol. 41, no. 7, pp. 1672–1675, Apr. 2016.
- [24] C. N. Alexeyev, T. A. Fadeyeva, B. P. Lapin, and M. A. Yavorsky, "Generation and conversion of optical vortices in long-period twisted elliptical fibers," *Appl. Opt.*, vol. 51, no. 10, p. C193, Apr. 2012.
- [25] C. N. Alexeyev, "Generation of optical vortices in spun multihelicoidal optical fibers," *Appl. Opt.*, vol. 51, no. 25, pp. 6125–6129, Sep. 2012.
- [26] H. X. Xu and L. Yang, "Conversion of orbital angular momentum of light in chiral fiber gratings," *Opt. Lett.*, vol. 38, no. 11, pp. 1978–1980, Jun. 2013.
- [27] C. N. Alexeyev, A. N. Alexeyev, B. P. Lapin, G. Milione, and M. A. Yavorsky, "Spin-orbit-interaction-induced generation of optical vortices in multihelicoidal fibers," *Phys. Rev. A, Gen. Phys.*, vol. 88, no. 6, Dec. 2013, Art. no. 063814.
- [28] G. Yin, Y. Wang, and C. Liao, "Long period fiber gratings inscribed by periodically tapering a fiber," *IEEE Photon. Technol. Lett.*, vol. 26, no. 7, pp. 689–701, Apr. 11, 2014.
- [29] Z. Li, S. Liu, and Z. Bai, "Residual-stress-induced helical long period fiber gratings for sensing applications," *Opt. Exp.*, vol. 26, no. 18, pp. 24113–24122, Sep. 2018.
- [30] C. Fu, Y. Wang, and S. Liu, "Transverse-load, strain, temperature, and torsion sensors based on a helical photonic crystal fiber," *Opt. Lett.*, vol. 44, no. 8, pp. 1984–1987, Apr. 15, 2019.



CAILING FU was born in Hubei, China, in 1989. She received the M.S. degree in optical engineering from the Wuhan Institute of Technology, Wuhan, China, in 2015, and the Ph.D. degree in optical engineering from Shenzhen University, Shenzhen, China, in 2018. From 2018 to 2020, she was with Shenzhen University, as a Postdoctoral Research Fellow, where she has been an Assistant Professor, since 2020. Her current research interests include optical fiber gratings and optical fiber sensors.



PENGFEI LI was born in Henan, China, in 1991. She received the B.S. degree from the School of Physics and Engineering, Henan University of Science and Technology, in 2016. She is currently pursuing the Ph.D. degree with Shenzhen University, China. Her current research interests include fiber Bragg gratings, femtosecond laser micro-machining, and optical fiber distributed sensing technology.



ZHIYONG BAI received the B.S. degree in physics from Ningbo University, Ningbo, China, in 2008, the M.S. degree in optics from South China Normal University, Guangzhou, China, in 2011, and the Ph.D. degree in optics from Nankai University, Tianjin, China, in 2014. From 2014 to 2015, he was with State Grid Electric Power Research Institute, as a Research and Development Engineer. Since 2015, he has been a Postdoctoral Research Fellow with the Guangdong and Hong Kong Joint Research Centre for Optical Fiber Sensors, Shenzhen University, Shenzhen, China. He is currently the author or coauthor of more than 30 journal articles. His current research interests include optical fiber gratings, orbital angular momentum, and optical fiber sensors.



YIPING WANG (Senior Member, IEEE) was born in Chongqing, China, in 1971. He received the B.Eng. degree in precision instrument engineering from the Xi'an University of Technology, Xi'an, China, in 1995, and the M.S. and Ph.D. degrees in optical engineering from Chongqing University, Chongqing, China, in 2000 and 2003, respectively.

From 2003 to 2005, he was with Shanghai Jiao Tong University, Shanghai, China, as a Postdoctoral Fellow. From 2005 to 2007, he was with The Hong Kong Polytechnic University, as a Postdoctoral Fellow. From 2007 to 2009, he was with the Leibniz Institute of Photonic Technology, Jena, Germany, as a Humboldt Research Fellow. From 2009 to 2011, he was with the Optoelectronics Research Centre, University of Southampton, Southampton, U.K., as a Marie Curie Fellow. Since 2012, he has been with Shenzhen University, Shenzhen, China, as a Distinguished Professor. He has authored or coauthored one book, 21 patent applications, and more than 240 journal and conference papers. His current research interests include optical fiber sensors, fiber gratings, and photonic crystal fibers. He is currently a Senior Member of the Optical Society of America and the Chinese Optical Society.